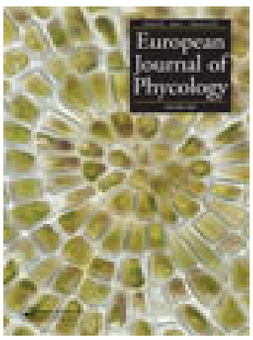

European Journal of Phycology

ISSN: 0967-0262 (Print) 1469-4433 (Online) Journal homepage: http://www.tandfonline.com/loi/tejp20

Photoacclimation and photoregulation strategies of *Corallina* (Corallinales, Rhodophyta) across the NE Atlantic

Christopher J. Williamson, Rupert Perkins, Marian L. Yallop, César Peteiro, Noemí Sanchez, Karl Gunnarsson, Maggie Gamble & Juliet Brodie

To cite this article: Christopher J. Williamson, Rupert Perkins, Marian L. Yallop, César Peteiro, Noemí Sanchez, Karl Gunnarsson, Maggie Gamble & Juliet Brodie (2018): Photoacclimation and photoregulation strategies of *Corallina* (Corallinales, Rhodophyta) across the NE Atlantic, European Journal of Phycology, DOI: 10.1080/09670262.2018.1442586

To link to this article: https://doi.org/10.1080/09670262.2018.1442586

EUROPEAN JOURNAL OF PHYCOLOGY, 2018
https://doi.org/10.1080/09670262.2018.1442586

Photoacclimation and photoregulation strategies of *Corallina* (Corallinales, Rhodophyta) across the NE Atlantic

Christopher J. Williamson[a,b], Rupert Perkins[c], Marian L. Yallop[b], César Peteiro [d], Noemí Sanchez[e], Karl Gunnarsson[f], Maggie Gamble[b] and Juliet Brodie[a]

[a]The Natural History Museum, Department of Life Sciences, Cromwell Road, London SW7 5BD, UK; [b]School of Biological Sciences, Life Sciences Building, University of Bristol, 24 Tyndall Avenue, Bristol BS8 1TQ, UK; [c]School of Earth and Ocean Sciences, Cardiff University, Cardiff CF10 3AT, Glamorgan, UK; [d]Instituto Español de Oceanografia (IEO), Centro Oceanográfico de Santander, Promontorio de San Martín, 39004 Santander, Spain; [e]Universitat de Girona (UdG), Facultat de Ciències, Campus de Montilivi s/n., 17071 Girona, Spain; [f]Marine Research Institute, Skúlagata 4, PO Box1390, 121 Reykjavik, Iceland

ABSTRACT

This study characterizes the photoacclimation and photoregulation mechanisms that allow calcified macroalgae of the genus *Corallina* (Corallinales, Rhodophyta) to dominate rock pool habitats across the NE Atlantic despite the highly variable irradiance regimes experienced. Rapid light curves (RLCs) were performed with pulse amplitude modulation (PAM) fluorometry *in situ* across a full seasonal cycle in the UK intertidal with *C. officinalis* and *C. caespitosa*. Latitudinal comparisons were performed across the full extent of *C. officinalis*' range in the NE Atlantic (Iceland–northern Spain), and for *C. caespitosa* in northern Spain. *Ex situ* RLCs with dark recovery were further employed to assess the optimal, as compared with actual, photophysiology across seasons and latitudes. *Corallina* species were shown to photoacclimate at seasonal timescales to changing irradiance, increasing light-harvesting during low-light autumn/winter periods and protecting photosystems during high-light summer conditions. Seasonal photoacclimation was achieved through alteration in the number of photosystem (PS) units (PSII and light harvesting antennae) over time. Non-photochemical quenching (NPQ) served as an important photoregulation mechanism utilized by *Corallina* to prevent or minimize photoinhibition over shorter time scales (seconds–hours), though the efficiency of NPQ was dependent on the seasonal-acclimated state. With increasing latitude the efficiency of photoregulation decreased, representing potential differential photoadaptation of *Corallina* across species ranges in the NE Atlantic. In contrast, highly conserved inter-specific patterns in photophysiological responses to irradiance were apparent. This study demonstrates the photophysiological mechanisms allowing *Corallina* to optimize use of the variable irradiance conditions apparent in rock pool environments, when and how they are employed, and their limitations.

ARTICLE HISTORY Received 18 September 2017; revised 15 January 2018; accepted 19 January 2018

KEY WORDS *Corallina*; NE Atlantic; NPQ; photoacclimation; photoregulation; rapid light curve

Introduction

Irradiance is an essential, yet highly variable, resource for macroalgal growth and survival (Henley & Ramus, 1989). In the intertidal, fluctuations in irradiance occur over a variety of time scales, ranging from seconds or less, to diurnal and seasonal-scale variations that are both predictable (changes in daylength and solar angle) and unpredictable (cloudiness, turbidity and run-off) (Dera & Gordon, 1968; Henley & Ramus, 1989; Lobban & Harrison, 1994). Intertidal species must cope with large gradients in irradiance that depend on both the daily course of solar irradiance, and the tidal range and temporal coincidence of maximum irradiance at mid-day with the timing of low tide (Goss & Jakob, 2010). For a benthic macroalga in a fixed position in the intertidal zone, the challenge is therefore to optimize the use of the variable irradiance regime experienced (Henley & Ramus, 1989).

To complicate this further, the quantity of photosynthetically active radiation (PAR, c. 400–700 nm) experienced by intertidal macroalgae is often in excess of that needed to saturate photosynthesis, particularly during summer periods (Franklin & Forster, 1997). In most intertidal macroalgae, the photochemical apparatus operates to optimize photosynthesis at low light levels associated with immersion, with the result that emersed plants are exposed to a large excess of light energy (Davison & Pearson, 1996). An excess of absorbed light energy can result in photo-damage to the photosynthetic apparatus (Hänelt *et al.*, 1993), leading to photo-oxidative damage via increased production of reactive oxygen species, which in extreme cases can cause pigment bleaching and death (Müller *et al.*, 2001). As such, intertidal macroalgae must respond to changes in irradiance in a manner that both optimizes photosynthesis and growth, whilst controlling for potential stress (Müller *et al.*, 2001).

Three general processes allow algae to manage prevailing irradiance conditions: adaptation, acclimation and regulation (Huot & Babin, 2011). Photoadaptation

CONTACT Christopher J. Williamson c.williamson@bristol.ac.uk

Published online 17 May 2018

is a long-term selection process in response to irradiance, ultimately resulting in genetically different ecotypes (Huot & Babin, 2011; Beer *et al.*, 2014). In contrast, photoacclimation refers to a phenotypic plastic response to a change in irradiance (Huot & Babin, 2011; Beer *et al.*, 2014). This is typically achieved by either an alteration of the size or number of photosynthetic units (photosystem II (PSII) and associated antennae pigments) (Falkowski & LaRoche, 1991; Müller *et al.*, 2001; Beer *et al.*, 2014). During short-term (seconds to hours) irradiance fluctuations, photoregulation further serves to provide a photo-protective network that allows photosynthetic efficiency to be rapidly tuned by safely dissipating excess absorbed light energy as heat and/or the excitation energy to be balanced within PSs to prevent or lower potential damage (Huot & Babin, 2011; Lavaud & Lepetit, 2013). Non-photochemical quenching (NPQ) is one mechanism of photoregulation that quenches photochemistry through non-photochemical processes, e.g. conversion of many of the excitations in the antennae complex to heat (Consalvey *et al.*, 2005). During NPQ, the light-driven de-epoxidation of specific xanthophyll pigments (typically violaxanthin, antheraxanthin and zeaxanthin) and the dark recovery of the initial pool, termed the xanthophyll cycle, is associated with thermal energy dissipation (Demmig-Adams & Adams, 1996; Esteban *et al.*, 2009; Goss & Jakob, 2010).

This study addresses the photophysiology of two intertidal macroalgae of the genus *Corallina* (Corallinales, Rhodophyta) across the NE Atlantic, namely *Corallina officinalis* Linnaeus and *Corallina caespitosa* Walker, Brodie & Irvine. These calcified, geniculate (articulated) species form extensive turfs that cover large areas of the intertidal and provide substratum, habitat and refugia for a number of important marine organisms (Johansen, 1981; Coull & Wells, 1983; Kelaher, 2002, 2003; Hofmann *et al.*, 2012; Perkins *et al.*, 2016). However, they are predicted to be significantly vulnerable to future anthropogenic change, including warming seawater temperatures and ocean acidification (Hofmann *et al.*, 2012; Egilsdottir *et al.*, 2013; Noisette *et al.*, 2013). As such, much recent research has been aimed at gaining a better understanding of *Corallina* ecophysiology, particularly in the NE Atlantic (e.g. Brodie *et al.*, 2013, 2016; Williamson *et al.*, 2014*a*, 2014*b*, 2015, 2017; Perkins *et al.*, 2016). The aim of this study was to build on the initial work of Williamson *et al.* (2014*b*) in order to identify the suite of photoacclimation and photoregulation mechanisms that allow *Corallina* to optimize light use in the variable intertidal environment, thus contributing to their dominance of NE Atlantic rock pools, and to characterize the use of these mechanisms in space and time. Photophysiological assessments were performed *in situ* across a full seasonal cycle in the UK intertidal, and complemented with *ex situ* techniques under laboratory conditions. Latitudinal comparisons were further performed for *C. officinalis* across the full extent of the species' range in the NE Atlantic (Iceland–northern Spain, Williamson *et al.*, 2015), and for *C. caespitosa* in northern Spain.

Methods

Sampling sites

Seasonality in *C. officinalis* and *C. caespitosa* photophysiology was assessed *in situ* using rapid light response curves (RLCs, Perkins *et al.*, 2006) across a complete annual cycle at Combe Martin (CM), North Devon, UK (Table 1, Fig. 3), and complemented with *ex situ* RLC with dark recovery assessments. Combe Martin lies within the middle of *C. officinalis*' range in the NE Atlantic (Iceland–northern Spain), though is comparatively closer to the currently known northern edge (northern England) of *C. caespitosa* (Williamson *et al.*, 2015). Williamson *et al.* (2014*b*) previously assessed the photophysiology of both species in relation to tidal emersion in this site, and as such, tidal assessment was not repeated here. Combe Martin is a north-west facing rocky intertidal site, positioned within a relatively sheltered bay. *Corallina caespitosa* inhabits a narrow zone (c. 2 cm

Table 1. Site and sampling information.

	Site		
	Combe Martin UK	Þorlákshöfn ICE	Comillas NSP
Location	51°12'13N 4°2'19W	63°53'36N 21°23'45W	43°23'18N 4°17'21W
Tidal Range	MHWS–MLWS 9.2–0.68 (8.52) MHWN–MLWN 6.9–3.1 (3.8)	MHWS–MLWS 3–0.2 (2.8) MHWN–MLWN 2.3–1 (2.2)	MHWS–MLWS 4.7–0.2 (4.5) MHWN–MLWN 3.2–1.4 (1.8)
Sampling Dates			
Winter	27.01.12		
Spring	10.03.12		
Summer	20.06.12	17.07.12	13.08.13
Autumn	03.09.12	05.09.13	19.10.12
Species sampled	*C. officinalis* *C. caespitosa*	*C. officinalis*	*C. officinalis** *C. caespitosa*
Shore heights sampled	Upper (5.5)	Lower (1.5)	Upper (3.0)

**Corallina officinalis* is accessible only during summer in NSP.

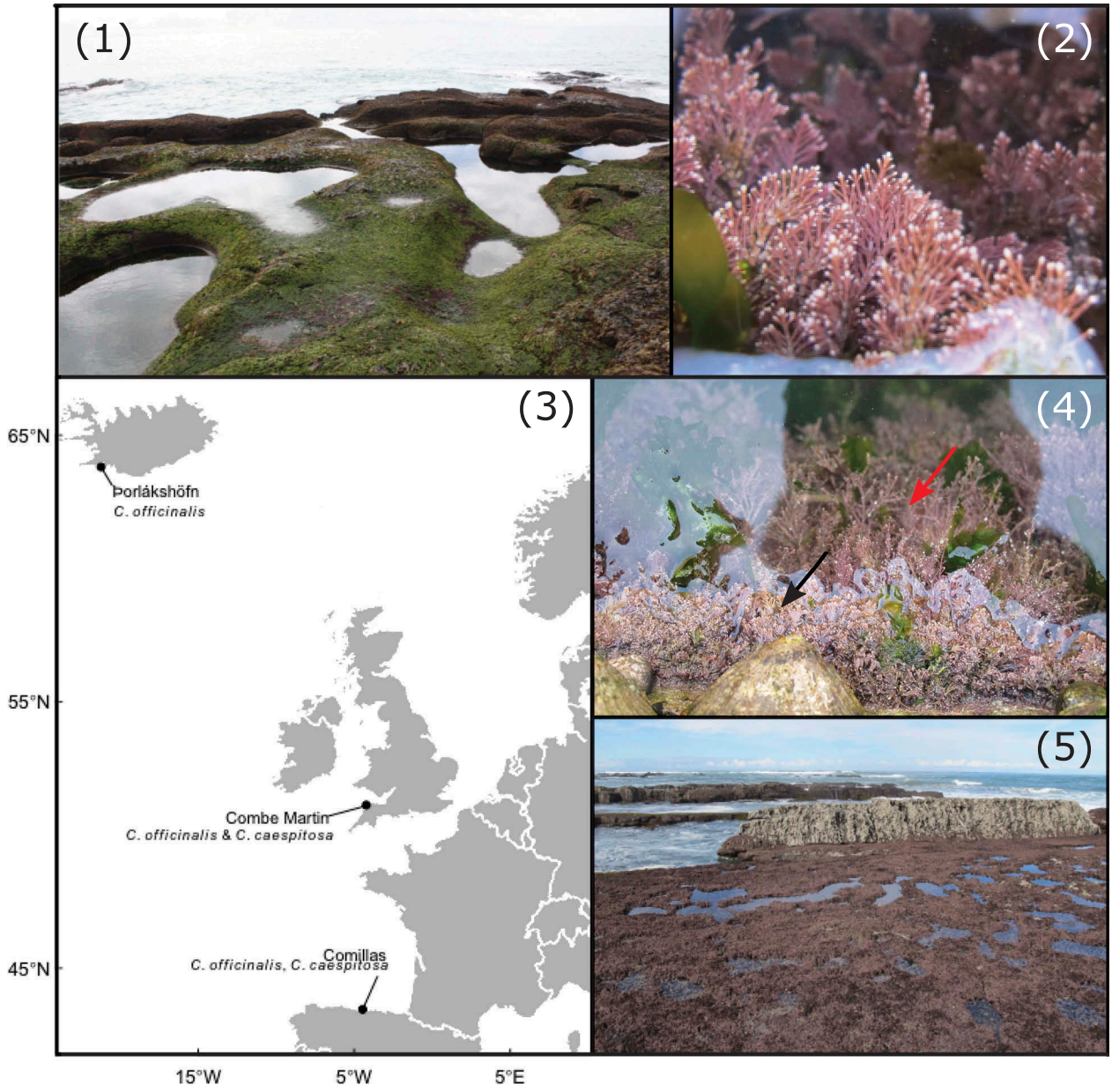

Figs. 1–5. Sampling sites, locations and species, showing: **Fig. 1.** intertidal rock pools at Þorlákshöfn, Iceland, dominated by **Fig. 2.** turfs of *C. officinalis*, **Fig. 3.** the locations of sampling sites across the NE Atlantic, **Fig. 4**. the upper layer of *C. caespitosa* (black arrow) in intertidal rock pools at Combe Martin, UK, with *C. officinalis* (red arrow) below, and **Fig. 5.** the well-developed turfing assemblage of corallines across the intertidal at Comillas, northern Spain.

deep) at the upper water line of large (c. 40 m^3, 0.5 m depth) upper shore rock pools created by a man-made walkway, with *C. officinalis* dominating below (Fig. 4). Across the lower intertidal, *C. officinalis* dominates rock pools and drainage channels, whilst *C. caespitosa* is absent.

Latitudinal patterns in *Corallina* photophysiology were further examined across the species' ranges in the NE Atlantic, including sites in Iceland and northern Spain (Fig. 3). *In situ* assessments of photophysiology were conducted for *C. officinalis* in Þorlákshöfn, SW Iceland (ICE, Fig. 1), during summer and autumn (Table 1), at the start, middle and end of daytime tidal emersion, with *ex situ* analyses performed in all sampling months. *Corallina officinalis* is the sole *Corallina* species found in Icelandic rock pools, and is present as a well-developed turf in rock pools at Þorlákshöfn (Figs 1, 2). In Comillas, northern Spain (NSP, Fig. 5), an exposed north-facing rocky shore is covered by a well-developed *Corallina* and *Ellisolandia* assemblage. *Corallina caespitosa* occupies very shallow (c. 2 cm deep) water covered areas of the intertidal whereas *C. officinalis* is a typically subtidal species, restricted to the intertidal in large rock pools (c. >1 m deep), found only in small patches accessible on spring tides (Fig. 5). *In situ* photophysiology assessments were therefore conducted for both species at their respective positions on shore during summer in NSP (Table 1), though for only *C. caespitosa* during autumn, as *C. officinalis*

was not accessible. In situ assessments were made across daytime tidal emersion and complemented with *ex situ* assessments.

In situ *photophysiology*

In the UK, RLCs were performed on $n = 5$ randomly selected *Corallina* fronds of each species immediately at the start of tidal emersion periods. Given tidal impacts to *Corallina* photophysiology demonstrated previously at this location (Williamson *et al.* 2014*a*), RLCs were performed at the start of tidal emersion periods to minimize influences on seasonal patterns. The order of RLC determination was further randomized across species to minimize potential diurnal effects. For photophysiology assessment in ICE, RLCs were performed after Williamson *et al.* (2014*a*) on $n = 3$ fronds randomly selected from each of three upper shore rock pools, at the start, middle and end of daytime tidal emersion. Start and end emersion periods were defined as being within 1.5 h of tidal isolation (start) and tidal reconnection (end) of the rock pool to the main tidal water mass. Middle emersion was the midway between these time points. In NSP, RLCs were performed on $n = 3$ fronds of *C. caespitosa* at the start, middle and end of tidal emersion, and $n = 3$ fronds of *C. officinalis* at the start and middle of emersion only, given the shorter duration of access to *C. officinalis* at its lower position on shore at this latitude.

In all cases, RLCs were performed on apical frond regions to avoid potentially self-shaded regions (Perkins *et al.*, 2016), and on the side of fronds facing direct sunlight, as the underside of fronds probably demonstrate different states of photoacclimation. RLCs were performed using a Walz Water-PAM fluorometer using a saturating pulse of c. 8600 µmol photons m^{-2} s^{-1}, for 800 ms duration, and with nine 30 s incrementally increasing light steps from 0 to 1944 µmol photons m^{-2} s^{-1}. Light step duration was selected to balance potential photoregulation occurring during longer light steps (60 s), with errors associated with shorter light steps (10 s) when samples have been exposed to high irradiance (Perkins *et al.*, 2006). Ambient photosynthetically active radiation (PAR, µmol photons m^{-2} s^{-1}) and rock pool water temperatures were monitored in parallel to *in situ* RLCs at 30 min intervals using a 2-pi LI-COR cosine-corrected quantum sensor positioned c. 5 cm above the surface of rock pools, and a digital thermometer (accuracy ±0.1°C), respectively. For each PAR measurement, a 15 s average was taken using an automated function on the sensor.

Ex situ *photophysiology assessment*

Ex situ assessment of *Corallina* photophysiology was performed during the present study to allow determination of photoacclimation and photoregulation dynamics under reduced influence of *in situ* abiotic conditions, facilitating identification of longer-term seasonal, latitudinal and inter-specific patterns in photochemistry. *Ex situ* RLCs with dark recovery phase were performed for $n = 3$ *C. officinalis* and *C. caespitosa* samples from CM during winter, summer and autumn, and for $n = 3$ samples of all species present at ICE and NSP during summer and autumn (Table 1). In all cases, 3 discrete samples of each *Corallina* species were sampled by hand from the intertidal at the end of tidal emersion. Samples were placed separately into 1 l containers containing site seawater obtained from rock pools at the time of sampling and transported immediately in darkness to nearby laboratory facilities. In the laboratory, samples were left submerged in site seawater in 1 l aquaria for a further 1 h in darkness to allow re-oxidation of Q_A, relaxation of NPQ and PSII repair (Ralph & Gademann, 2005); seawater was replenished every 0.5 h to maintain aeration and ambient site temperatures (Table 3). Following the 1 h dark adaptation period, *ex situ* RLCs with recovery were performed on an apical frond region of each sample. RLCs were performed as *in situ*, with recovery of photochemistry subsequently tracked over a 17.5 min period of darkness using the Walz Water-PAM inbuilt programme for recovery phase, with quantum efficiency measurements at 10, 40, 100, 160, 460 and 1060 s.

Data treatment

To avoid long periods of dark-adaptation prior to *in situ* RLCs, which would lead to modification of the photoacclimation state of the cells investigated (Ralph & Gademann, 2005; Perkins *et al.*, 2010), the maximum light utilization efficiency for *in situ* RLCs (F_v/F_m) was calculated from F_m and F_o values obtained during the initial RLC step of 30 s darkness (see Table 2 for fluorescence parameter definitions and derivations). For *ex situ* RLCs, full dark adaptation was apparent, though F_v/F_m was also calculated as above. Electron transport through PSII was calculated from all RLCs in relative units (*rETR*), assuming an equal division of PAR between PSI and PSII. Analysis of all RLCs (*rETR* vs. PAR) followed Perkins *et al.* (2006), with iterative curve fitting using the 'nls' function of R base package (R Core Team, 2014) and calculation of the relative maximum electron transfer rate ($rETR_{max}$), the maximum light utilization coefficient (α) and the light saturation coefficient (E_k) following Eilers & Peeters (1988). Down-regulation in the form of Stern–Volmer non-photochemical quenching (NPQ) was calculated from the quenching of the maximum fluorescence yield (i.e. the reduction from the dark-adapted maximum yield, F_m, to the operational maximum yields in the light, F_m'). Given the short dark-adaptation period applied

Table 2. Fluorescence parameters, definitions and derivations (after Cosgrove & Borowitzka, 2011).

Parameter	Definition	Derivation
F_o	Minimum fluorescence yield (dark adapted, all RCIIs open)	
F_m	Maximum fluorescence yield (dark adapted, all RCIIs open with no NPQ)	
F_v	Maximum variable fluorescence	F_m–F_o
F_v/F_m	Maximum quantum efficiency (dark adapted)	$(F_m–F_o)/F_m$
F'	Fluorescence yield in actinic light	
F_m'	Maximum fluorescence yield in actinic light	
$F_m'_m$	The maximum value of F_m'	
F_q'	Fluorescence quenched in actinic light	$F_m'–F'$
F_q'/F_m'	Effective quantum efficiency in actinic light	$(F_m'–F')–F_m'$
RQE	Relative quantum efficiency	$(F_q'/F_m')/(F_v/F_m) \times 100$
rETR	Relative electron transport rate (through PSII)	$F_q'/F_m' \times PAR \times 0.5$
NPQ	(Stern–Volmer) Non-photochemical quenching	$(F_m–F_m')/F_m'$
	Non-photochemical quenching calculated with the maximum value of F_m' ($F_m'_m$) after Serôdio *et al.* (2005)	$(F_m'_m–F_m')/F_m'$

All parameters are dimensionless (PAR = photosynthetically active radiation).

during *in situ* RLCs (30 s), fluorescence quenching was observed in the dark-adapted state (i.e. $F_m' > F_m$) and thus *in situ* NPQ was calculated using the maximum F_m' value ($F_m'_m$) after Serôdio *et al.* (2005). Two NPQ parameters were subsequently calculated for each *in situ* RLC; NPQ at the initial RLC step (NPQ_{RESID}), representing residual NPQ due to *in situ* irradiance, and NPQ at the final RLC step (NPQ_{INDUC}) representing the amount of NPQ induced by the RLC itself. Given the long dark-adaptation period prior to *ex situ* RLCs, fluorescence quenching in the dark-adapted state was not observed and thus typical Stern–Volmer NPQ was calculated using F_m. Quantum efficiency as a proportion of F_v/F_m (the relative quantum efficiency, RQE) was calculated for each *ex situ* RLC step and dark recovery measurement to allow comparison of induction and recovery dynamics across seasons, species and latitudes.

Data analysis

All statistical analyses and plotting of data were performed using R v.3.0.2 (R Core Team, 2014). Prior to all analyses, normality of data was tested using the Shapiro–Wilk test and examination of frequency histograms. If data were not normally distributed, Box–Cox power transformation was applied using the boxcox function of the MASS package (Venables & Ripley, 2002), and normality re-checked. Following the application of models to data, model assumptions were validated by examination of model criticism plots. Statistical comparisons of RLC (and recovery) parameters between independent variables were performed where appropriate using either t-test, analysis of variance (ANOVA), or linear mixed-effects models (LMER) with restricted maximum likelihood (REML) criterion (Bates *et al.*, 2013), as detailed below.

Seasonal photophysiology in the UK

Differences in ambient irradiance and water temperature between sampling months at CM (Table 1) were analysed by 1-way ANOVA with the factor month (4 levels). Seasonal and interspecific differences in *in situ* photophysiological parameters were analysed using 2-way ANOVA with the factors month (4 levels) and species (2 levels), and interaction term. *Ex situ* photophysiology was analysed using 1-way ANOVA with the factor season for *C. officinalis* (3 levels), and t-test analysis with the factor season (2 levels) for *C. caespitosa*.

ICE and NSP latitudinal comparisons

For ICE data, differences in ambient irradiance between seasons and over tidal emersion periods were examined using 2-way ANOVA with the factors season (2 levels) and tide (3 levels), and interaction term. Rock pool water temperatures and *in situ* photophysiological parameters from ICE were analysed using LMER with the fixed factors season (2 levels) and tide (3 levels), and rock pool (3 levels) as random term. *Ex situ* photophysiology was analysed using *t*-test comparisons of parameters in relation to season (2 levels). For NSP data, irradiance and water temperature were examined using 2-way ANOVA with the factors season (2 levels) and tide (3 levels), and interaction term. *Corallina caespitosa in situ* photophysiology was analysed using 2-way ANOVA with the factors season (2 levels) and tide (3 levels) and interaction, and interspecific comparisons with *C. officinalis* at start and middle summer tidal emersion achieved with 1-way ANOVA with the factor species (2 levels), and tide as random term (2 levels). NSP *C. caespitosa ex situ* photophysiological parameters were examined between seasons using *t*-test with the factor season (2 levels).

Results

Seasonal photochemistry of UK Corallina

Ambient irradiance and rock pool water temperatures ranged from 270±16 to 1143±124 µmol photons m^{-2} s^{-1}, and 7.7±0.4 to 19.2±0.9°C during sampling at Combe Martin (CM), respectively, with significantly

increased irradiance ($F_{3,16}$ = 116.06, P < 0.01) and water temperature ($F_{3,16}$ = 42.04, P < 0.001) apparent during June and September as compared with January and March, and no difference between respective pairs of months (Table 3).

Strong seasonality in RLCs and derived parameters was apparent for both *C. officinalis* and *C. caespitosa* across sampling months at CM (Figs 6, 7, Supplementary table 1). From January to June, declines in *C. officinalis* F_v/F_m, $rETR_{max}$ and α, reflected increased photo-stress and corresponding suppression of photochemistry, with some recovery in September. Highly comparable patterns were also observed for *C. caespitosa*, though a more abrupt shift in parameters was evident between March and June in comparison with *C. officinalis* (Fig. 7). Although variable, E_k did not differ significantly between sampling months for either species. Ambient irradiance was less than E_k during January and March, suggesting light-limitation of photosynthesis. Conversely, ambient irradiance was c. 2.4- and 1.8-times E_k during June, and 3.6- and 2.5-times E_k during September, for *C. officinalis* and *C. caespitosa*, respectively, suggesting saturation and hence potential to induce photo-stress. No interspecific differences in F_v/F_m, $rETR_{max}$, α or E_k were observed during any sampling month.

Table 3. Mean (± SE) water temperature and irradiance measured at sites during RLC photophysiology assessments.

Site	Date	Season	Tidal period	Water temperature (°C)	Ambient irradiance (μmol photons m^{-2} s^{-1})
Combe	27.01.12	Winter	S	7.87±0.07	311±42
Martin,	10.03.12	Spring	S	7.72±0.41	270±16
UK	20.06.12	Summer	S	17.30±2.80	1111±267
	03.09.12	Autumn	S	19.24±0.91	1143±124
Þorlákshöfn,	17.07.12	Summer	S	15.05±0.03	712±83
Iceland			M	15.25±0.03	630±60
			E	15.57±0.07	616±66
	05.09.13	Autumn	S	9.66±0.08	861±76
			M	10.20±0.14	1152±63
			E	11.20±0.11	1215±70
Comillas,	13.08.13	Summer	S	20.94±0.27	1160±59
northern			M	22.68±0.19	1568±142
Spain			E	23.67±0.11	1405±344
	19.10.12	Autumn	S	18.68±0.07	500±29
			M	18.90±0.04	510±48
			E	18.94±0.04	264±24

S = start, M = middle and E = end tidal emersion.

Non-photochemical quenching (NPQ) varied between seasons for both *C. officinalis* and *C. caespitosa* (Fig. 7, Supplementary table 1). NPQ induced under *in situ* conditions was greatest during summer/autumn as demonstrated by increased NPQ_{RESID}, with minimal NPQ_{INDUC} apparent at the end of summer/autumn RLCs. The opposite trends were observed during winter, demonstrating minimal active NPQ under *in situ* conditions, but induction of NPQ by RLC irradiance. No significant interspecific differences in NPQ parameters were evident across months (Supplementary table 1).

In contrast to *in situ* photophysiology, no significant difference in *C. officinalis* or *C. caespitosa* $rETR_{max}$, α or E_k was evident between seasons as determined by *ex situ* RLCs with dark recovery (Fig. 8, Table 4,

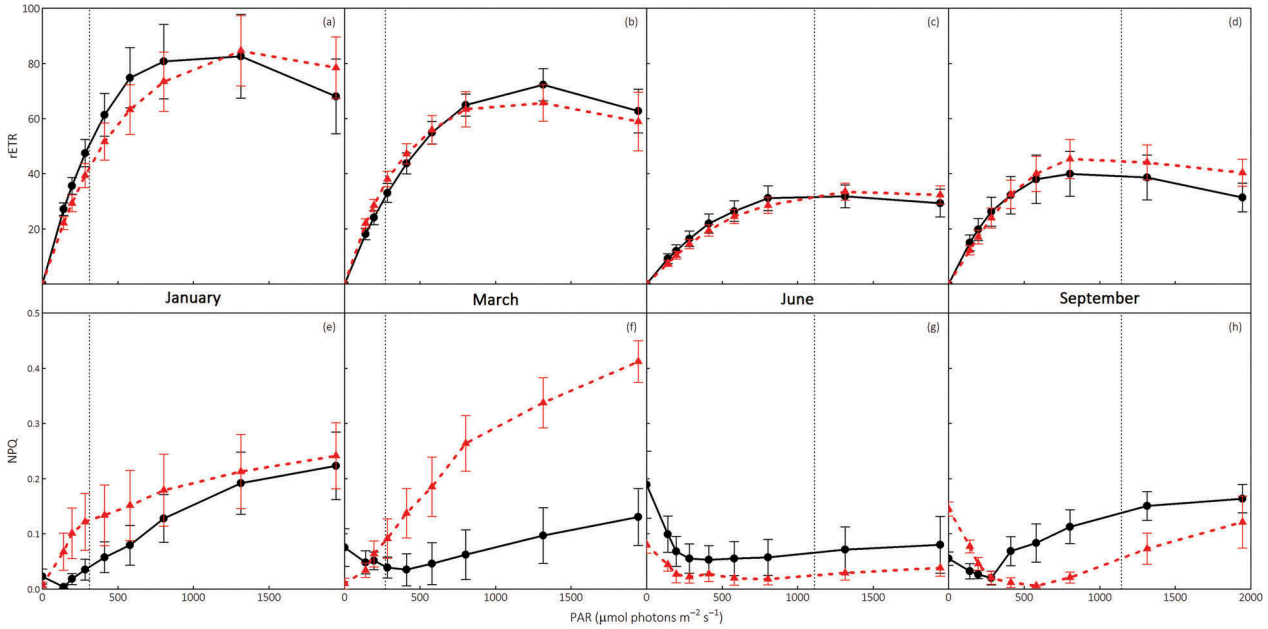

Fig. 6. *In situ* rapid light response curves (RLCs) of *C. officinalis* (circles and solid lines) and *C. caespitosa* (triangles and dashed lines) performed at Combe Martin, UK, during January, March, June and September, showing (a–d) relative electron transport rates (rETR) and (e–h) non-photochemical quenching (NPQ) across RLCs (mean ± SE, n = 5). Dotted vertical lines represent the average ambient irradiance recorded *in situ* at the time of RLC determination.

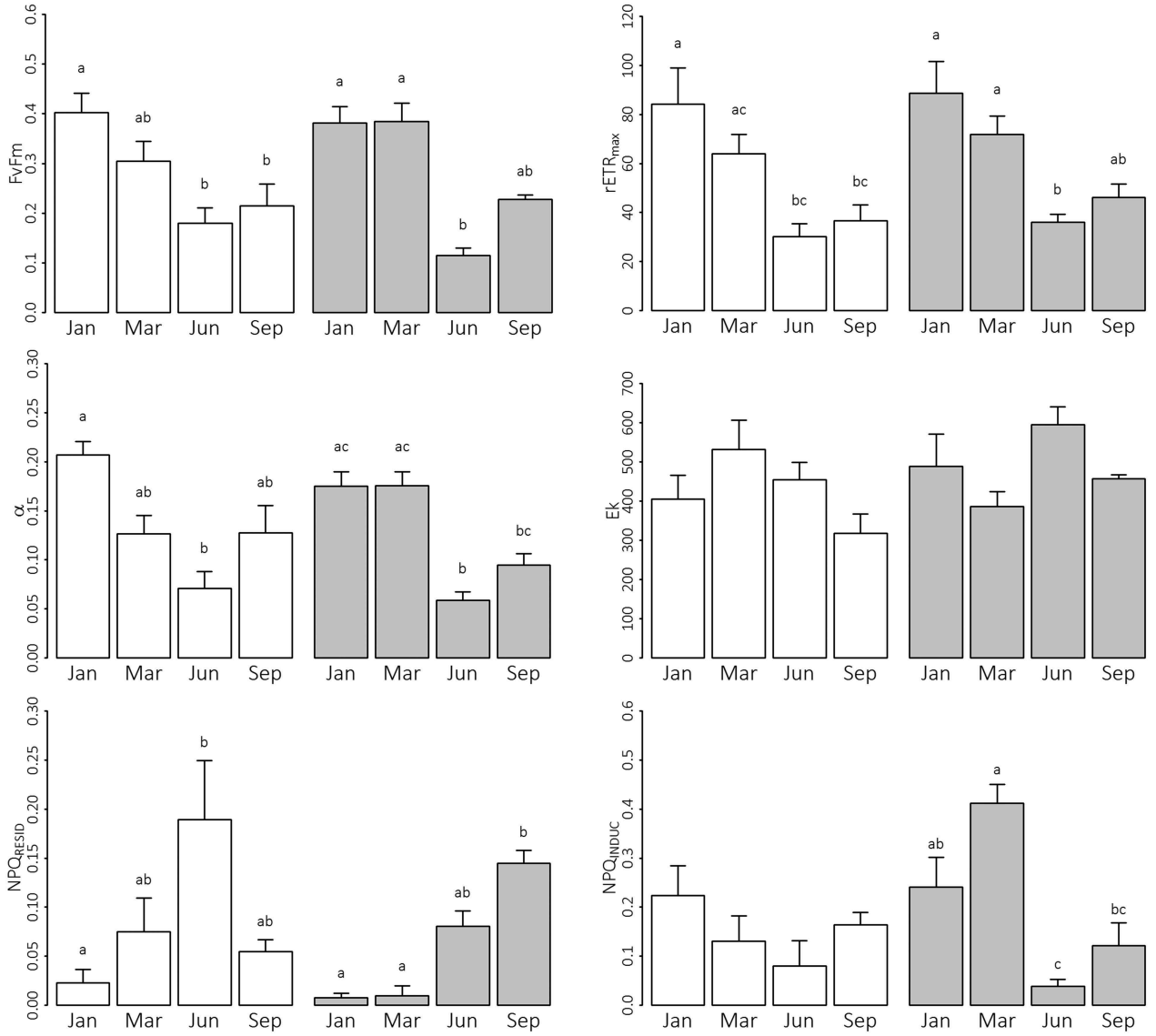

Fig. 7. Parameters determined from *in situ* rapid light response curves of *Corallina officinalis* (unshaded bars) and *C. caespitosa* (shaded bars) at Combe Martin, UK, during January (Jan), March (Mar), June (Jun) and September (Sep), showing: the maximum quantum efficiency in the dark adapted state (*Fv/Fm*), the relative maximum rate of electron transport (*rETRmax*), the light utilization efficiency (*α*), the light utilization coefficient (*Ek*), and non-photochemical quenching (NPQ) at the start- and end- of RLCs (mean ± SE, $n = 5$). Lower-case letters denote Tukey's HSD homogeneous subsets in relation to sampling month.

Supplementary table 2). F_v/F_m and NPQ_{INDUC} were significantly lower in summer as compared with autumn and winter for *C. officinalis*. Unfortunately, instrumentation failure prevented *ex situ* photophysiology assessment of *C. caespitosa* during summer. Relative quantum efficiency (RQE) decreased to 14.7 ±1.5% in *C. officinalis* and 14.9±0.9% in *C. caespitosa* at the end of *ex situ* RLCs, with no seasonal difference apparent for either species. The magnitude of dark recovery in RQE was greatest during summer (87.3 ±9.3%) and autumn (88.3±3.2%) in comparison with winter (60.1±6.8%) for *C. officinalis*, and during autumn (91.5±6.9%) in comparison with winter (55.9 ±6.1%) for *C. caespitosa*. NPQ relaxation during dark recovery was fastest during summer (160 s), then autumn (460 s), with slowest relaxation in winter (17.5 min) for *C. officinalis*. NPQ relaxation was faster overall for *C. caespitosa*, with similar seasonal dynamics (160 s in autumn, 460 s in winter).

Icelandic Corallina *photophysiology*

Irradiance was significantly lower during summer in ICE as compared with autumn, with no significant change in irradiance apparent over tidal emersion periods during either season ($F_{1,24} = 50.80$, $P < 0.001$) (Table 3). Rock pool water temperatures were significantly increased during summer as compared with autumn ($F_{1,24} = 6973.01$, $P < 0.001$), and significantly increased at the end of tidal emersion during both seasons ($F_{2,24} = 86.55$, $P < 0.001$).

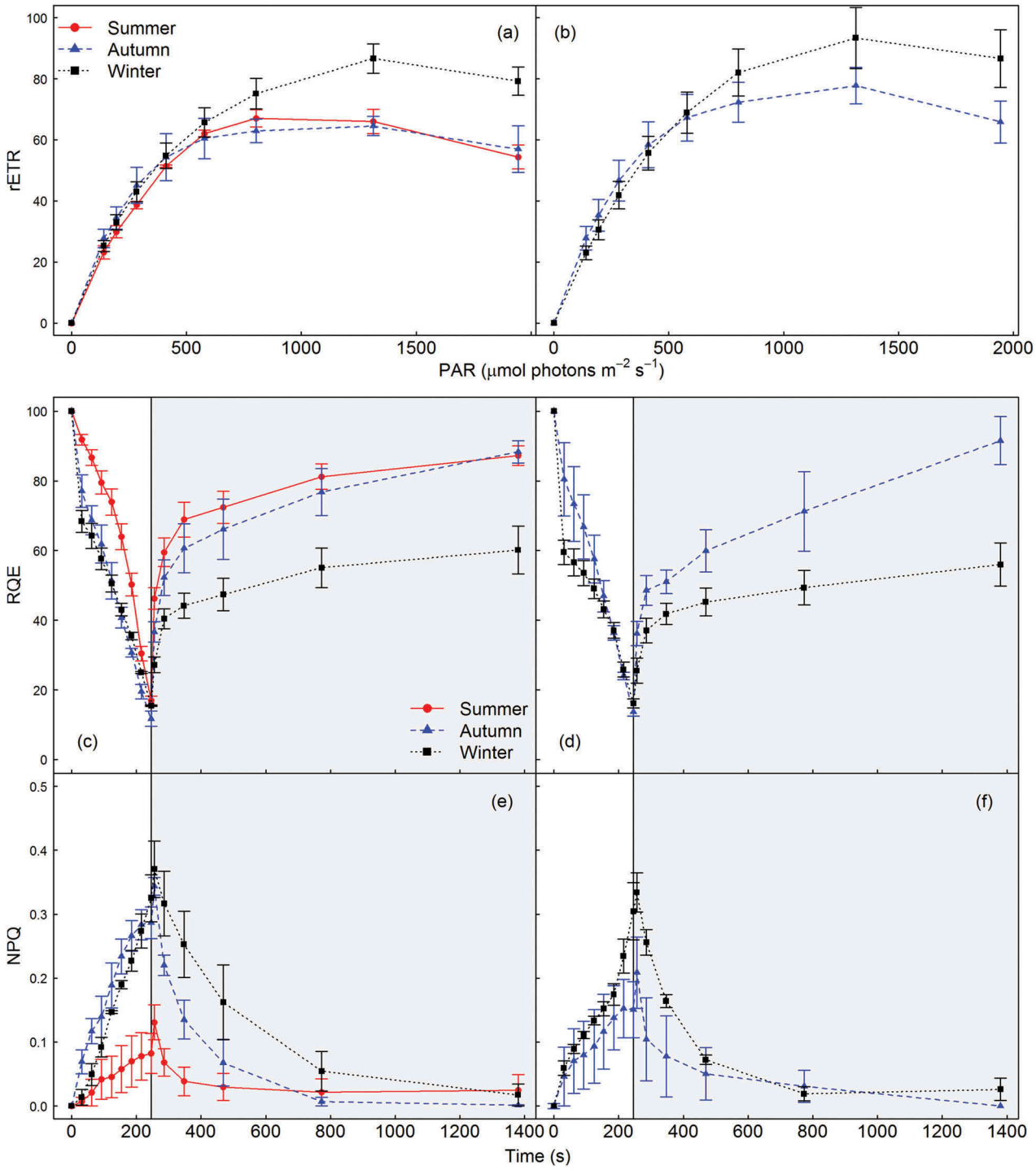

Fig. 8. *Ex situ* rapid light response curves (RLCs) with recovery for *Corallina officinalis* (left hand panels) and *C. caespitosa* (right hand panels) during summer (circles and solid lines), autumn (triangles and dashed lines) and winter (squares and dotted lines), from Combe Martin, UK. Showing (a & b) relative electron transport rates (rETR) over the induction phase of RLCs, and (c & d) relative quantum efficiency (RQE) and (e & f) non-photochemical quenching (NPQ) over the induction (white background) and dark recovery (grey background) phases (mean ± SE, n = 3).

Table 4. Mean *ex situ* photophysiology of UK *Corallina officinalis* and *C. caespitosa* across seasons as assessed by RLCs with recovery (n = 3 ± SE in parentheses).

	C. officinalis			*C. caespitosa*	
	Summer	Autumn	Winter	Autumn	Winter
RLC parameters					
F_v/F_m	0.36(0.06)	0.51(0.03)	0.53(0.02)	0.49(0.02)	0.55(0.03)
$rETR_{max}$	68.48(3.63)	71.68(4.08)	83.63(4.9)	77.95(4.84)	91.97(9.41)
α	0.17(0.02)	0.23(0.03)	0.2(0.02)	0.22(0.04)	0.17(0.02)
E_k	418.79(71.5)	320.09(59.7)	426.26(29.29)	377.42(66.18)	548.11(24.09)
	Relative Quantum Efficiency				
	Summer	Autumn	Winter	Autumn	Winter
Recovery parameters					
End RLC	17.02(4.16)	11.71(2.21)	15.48(0.19)	13.69(1.16)	16.14(1.26)
End dark	87.31(9.36)	88.33(3.23)	60.16(6.82)	91.54(6.9)	55.95(6.18)
	NPQ				
	Summer	Autumn	Winter	Autumn	Winter
End RLC	0.08(0.03)	0.29(0.02)	0.33(0.04)	0.15(0.04)	0.3(0.04)
End dark	0.02(0.02)	0(0)	0.02(0.02)	0(0)	0.03(0.02)

End RLC = relative quantum efficiency (%) or NPQ at the final RLC light step; End dark = the maximum recovery in relative quantum efficiency (%) and relaxation of NPQ achieved by the end of the dark recovery period.

At the seasonal resolution, F_v/F_m determined from *in situ* RLCs was greatest during autumn, whilst $rETR_{max}$ and α were significantly decreased as compared with summer (Fig. 9, Supplementary table 3). No seasonal difference in E_k was apparent, though ambient irradiance exceeded E_k suggesting light-saturated photosynthesis in both seasons. Greatest NPQ_{RESID} was observed during autumn, highlighting maximal active NPQ under *in situ* irradiance, whereas a greater capacity for NPQ was demonstrated during summer, given significantly increased NPQ_{INDUC} in comparison with autumn. Over tidal emersion periods, significant decreases in *C. officinalis* $rETR_{max}$ were apparent during both summer and autumn in ICE (Fig. 9, Supplementary table 3), though the onset and magnitude of decrease differed between seasons. During summer, $rETR_{max}$ was maintained until the end of tidal emersion, whereby it decreased to 63% of initial values. Conversely, $rETR_{max}$ was significantly decreased by mid emersion period during autumn, remaining low until the end of emersion, at 38% of the initial value. No other differences were observed in *C. officinalis* photophysiology over tidal emersion periods in ICE.

Ex situ RLCs with dark recovery differed from observations made *in situ* in ICE. No seasonal difference was apparent in *C. officinalis* F_v/F_m or $rETR_{max}$, while α was significantly increased, and E_k significantly decreased, during autumn in comparison with summer (Table 5, Supplementary fig. 1, Supplementary table 4). NPQ increased over the course of summer *ex situ* RLCs to 0.73±0.09, whilst NPQ plateaued at a light intensity of c. 580 µmol photons $m^{-2}\,s^{-1}$ during autumn, and remained constant to the end of RLCs at 0.43±0.10. In parallel, downturn in *rETR* across the last four light steps of autumn RLCs indicated photoinhibition. RQE at the final light step was decreased to 12.25±1.09% during summer in ICE and 5.70±0.18% during autumn (Table 5, Supplementary fig. 1). Rapid increase in RQE and relaxation of NPQ were observed during both seasons from 0 to 160 s of dark recovery. Over the final 15 min of recovery, however, NPQ remained active during summer, preventing full recovery of RQE. During autumn, relaxation of NPQ continued across the final 15 min of darkness to 0.04±0.03 by the end of recovery. RQE showed greater recovery during autumn than summer, but did not achieve 100% of initial values.

Northern Spanish Corallina *photophysiology*

Irradiance was significantly increased during summer as compared with autumn in NSP ($F_{1,42}$= 179.28, P < 0.001), though no significant change was apparent over tidal emersion during either season (Table 3). Similarly, rock pool water temperature was significantly increased during summer as compared with autumn in NSP ($F_{1,42}$ = 539.42, P < 0.001), and significantly increased over summer tidal emersion ($F_{2,42}$ = 35.13, P < 0.001).

Decreased F_v/F_m, *rETRmax* and α were observed for *in situ C. caespitosa* during summer as compared with autumn, indicating increased summer stress and reduced capacity for photosynthesis (Fig. 10, Supplementary table 5). E_k did not significantly differ between seasons, and was lower than ambient PAR for the duration of summer emersion, though greater than ambient PAR by the end of autumn emersion. For *C. caespitosa*, the requirement for active NPQ *in situ* was observed in both summer and autumn, with NPQ_{RESID} in the range of 0.2–0.4 across seasons, and consistently reduced NPQ_{INDUC} observed. During summer, *C. officinalis* F_v/F_m, $rETR_{max}$ and α were significantly increased as compared with *C. caespitosa*, suggesting reduced

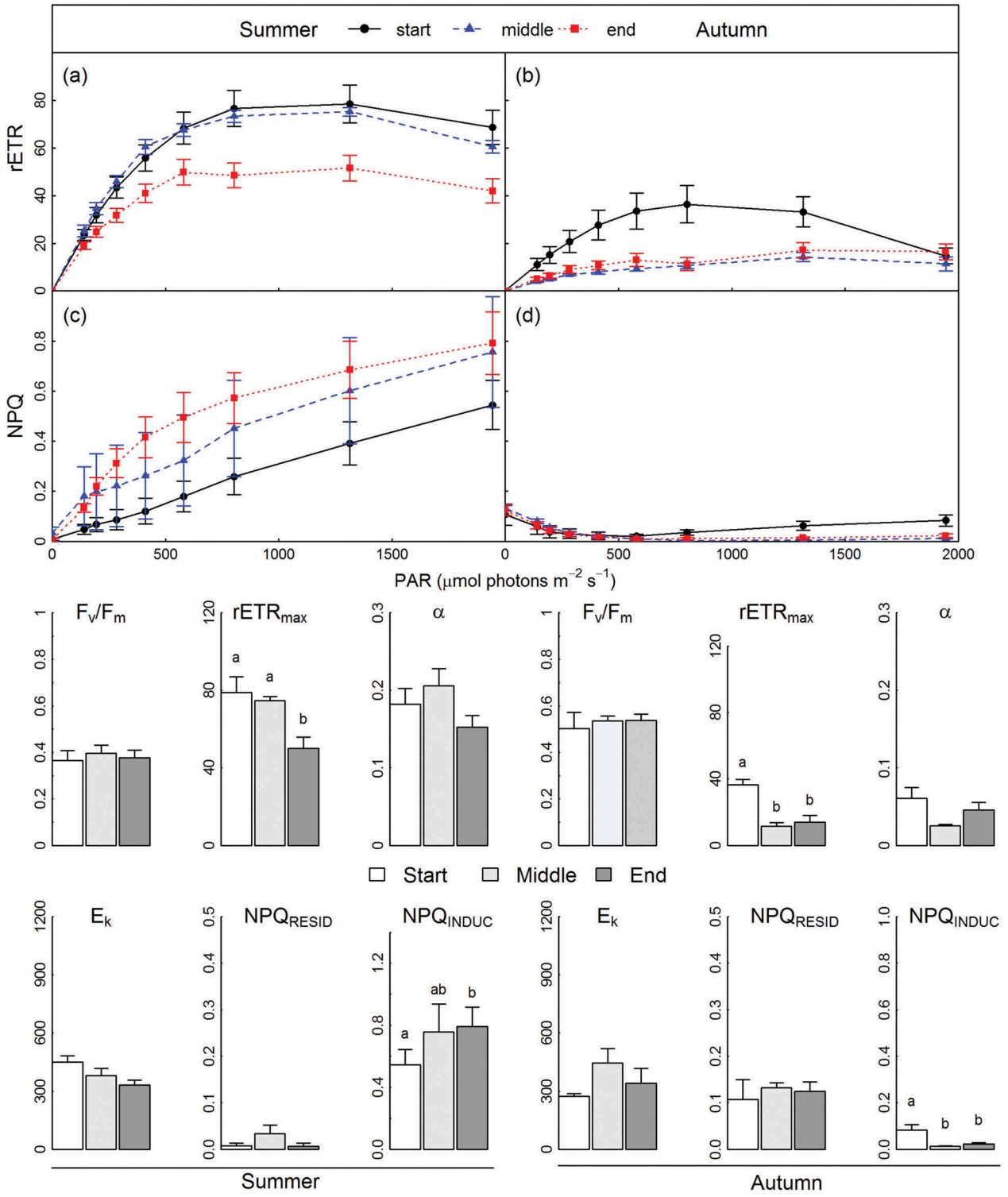

Fig. 9. *Corallina officinalis* photophysiology in Þorlákshöfn, Iceland, in summer (left hand panels) and autumn (right hand panels) at the start (circles and solid lines/unshaded bars), middle (triangles and dashed lines/light grey bars) and end (squares and dotted lines/dark grey bars) of tidal emersion periods. Upper panels show the relative electron transport rates (rETR) (a & b) and non-photochemical quenching (NPQ) (c & d) determined over RLCs, with parameters derived from RLCs shown in bar plots below (mean ± SE, n = 9). Lower case letters denote homogeneous subsets determined from Tukey's HSD analysis in relation to the factor 'tide'.

stress and a greater capacity for photosynthesis (Fig. 11, Supplementary table 6). No other species differences were apparent. No significant change in any photophysiological parameter was observed for either species across summer emersion in NSP, whilst during autumn, *C. caespitosa* demonstrated significantly decreased F_v/F_m and $rETR_{max}$ by the end of tidal emersion.

Corallina caespitosa F_v/F_m, $rETR_{max}$ and α determined from *ex situ* RLCs in NSP were significantly increased during autumn in comparison with summer, whilst E_k was not significantly different (Table 6,

Table 5. Icelandic *Corallina officinalis ex situ* photophysiology in summer and autumn, as assessed by RLCs with recovery (n = 3 ± SE in parentheses).

	Summer	Autumn		Summer	Autumn
RLC parameters					
F_v/F_m	0.40(0.03)	0.49(0.03)	$rETR_{max}$	45.70(6.92)	49.66(1.25)
α	0.09(0.03)	0.28(0.08)	E_k	561.17(111.74)	204.66(56.61)
	Relative Quantum Efficiency			NPQ	
	Summer	Autumn		Summer	Autumn
Recovery parameters					
End RLC	12.25(1.1)	5.71(0.18)	End RLC	0.73(0.1)	0.43(0.11)
End dark	61.18(3.02)	70.97(2.54)	End dark	0.36(0.08)	0.04(0.03)

End RLC = relative quantum efficiency (%) or NPQ at the final RLC light step; End dark = the maximum recovery in relative quantum efficiency (%) and relaxation of NPQ achieved by the end of the dark recovery period.

Supplementary fig. 2, Supplementary table 7). RQE at the end of *ex situ* RLCs did not differ between seasons for *C. caespitosa*, though at the end of the dark recovery phase (17.5 min), RQE remained below initial values (88.4±6.4%) during summer, whilst full recovery was evident during autumn. NPQ relaxed to 0 within 100–160 s of darkness for *C. caespitosa* during both seasons. *Ex situ* RLCs with recovery were performed in NSP for *C. officinalis* during summer only, preventing seasonal comparisons (Supplementary fig. 3). However, *C. officinalis* F_v/F_m, $rETR_{max}$, α and E_k were comparable to those determined for *C. caespitosa* during summer (Table 6). RQE decreased to 13.3±1.2% at the end of RLCs with NPQ increased to 0.17±0.03. During dark recovery, RQE did not achieve complete recovery, reaching 89.4±6.0% of initial values, while NPQ decreased to 0 after 17.5 min of darkness.

Discussion

This study has elucidated the photoacclimation and photoregulation mechanisms utilized by keystone *Corallina* species across the NE Atlantic, demonstrating (i) seasonal photoacclimation driven by alteration in the number of photosystem units, (ii) the importance of non-photochemical quenching in *Corallina* photoregulation, (iii) decreased capacity of high latitude populations to photoregulate, and (iv) conserved interspecific patterns in photochemistry. Our data provide a significant advance in our understanding of the ability of *Corallina* to optimize use of the highly variable irradiance apparent in rock pool environments. By contrasting *in situ* with *ex situ* dynamics, we were further able to distinguish differences between actual versus optimal photochemistry, facilitating comparisons between seasons, across latitudes, and between species.

Seasonal photoacclimation to irradiance

Seasonal acclimation of photochemistry was apparent for both *Corallina* species at all latitudes examined during the present study, with both *in situ* and *ex situ* data indicating increased light-harvesting capability under low-light autumn/winter conditions, and down-regulation of photochemistry under high-light summer conditions. Photoacclimation can be achieved through either a change in the size or number of photosynthetic units (PSU) (Ramus, 1981; Richardson *et al.*, 1983; Falkowski & LaRoche, 1991; Beer *et al.*, 2014). Under low-light conditions, an increase in PSU size is reflected by an increase in light utilization efficiency (α), but a decrease in maximal productivity (P_{max} or ETR_{max}) (Richardson *et al.*, 1983; Beer *et al.*, 2014). Conversely, with photoacclimation to low irradiance via increase in PSU number, both antenna size and reaction centre numbers per cell increase in concert, such that all aspects of the photosynthetic functional apparatus are enhanced as light for growth is decreased (Beer *et al.*, 2014). Given that both α and $rETR_{max}$ of *C. officinalis* and *C. caespitosa* varied inversely with irradiance across seasons in the UK intertidal, data indicated that photoacclimation was achieved through alteration of PSU number, as opposed to size, allowing maximum light utilization during low-light winter periods. These findings were supported by seasonal dynamics in photophysiology assessed over tidal emersion periods in the UK by Williamson *et al.* (2014*a*), and during the present study in northern Spain. Data are thus consistent with previous designation of *Corallina* as being effective at harvesting and utilizing irradiance at low intensities (Häder *et al.*, 1997, 2003).

Opposite seasonal dynamics in photophysiology observed *in situ* in Iceland (i.e. increased α and $rETR_{max}$ during summer as compared with autumn) were an artefact of the irradiance apparent during field sampling, as opposed to differential seasonal photoacclimation at this latitude. During autumn, high irradiance was apparent during field sampling in Iceland, to levels greater than during summer. Under these conditions, *C. officinalis* $rETR_{max}$ and α were significantly decreased, with active NPQ *in situ* highlighted by increased NPQ_{RESID}. Whilst photoregulation via NPQ can prevent long-lasting damage to photosynthetic components by diversion of excess energy as heat (Franklin & Forster, 1997; Consalvey *et al.*, 2005; Lavaud & Lepetit, 2013),

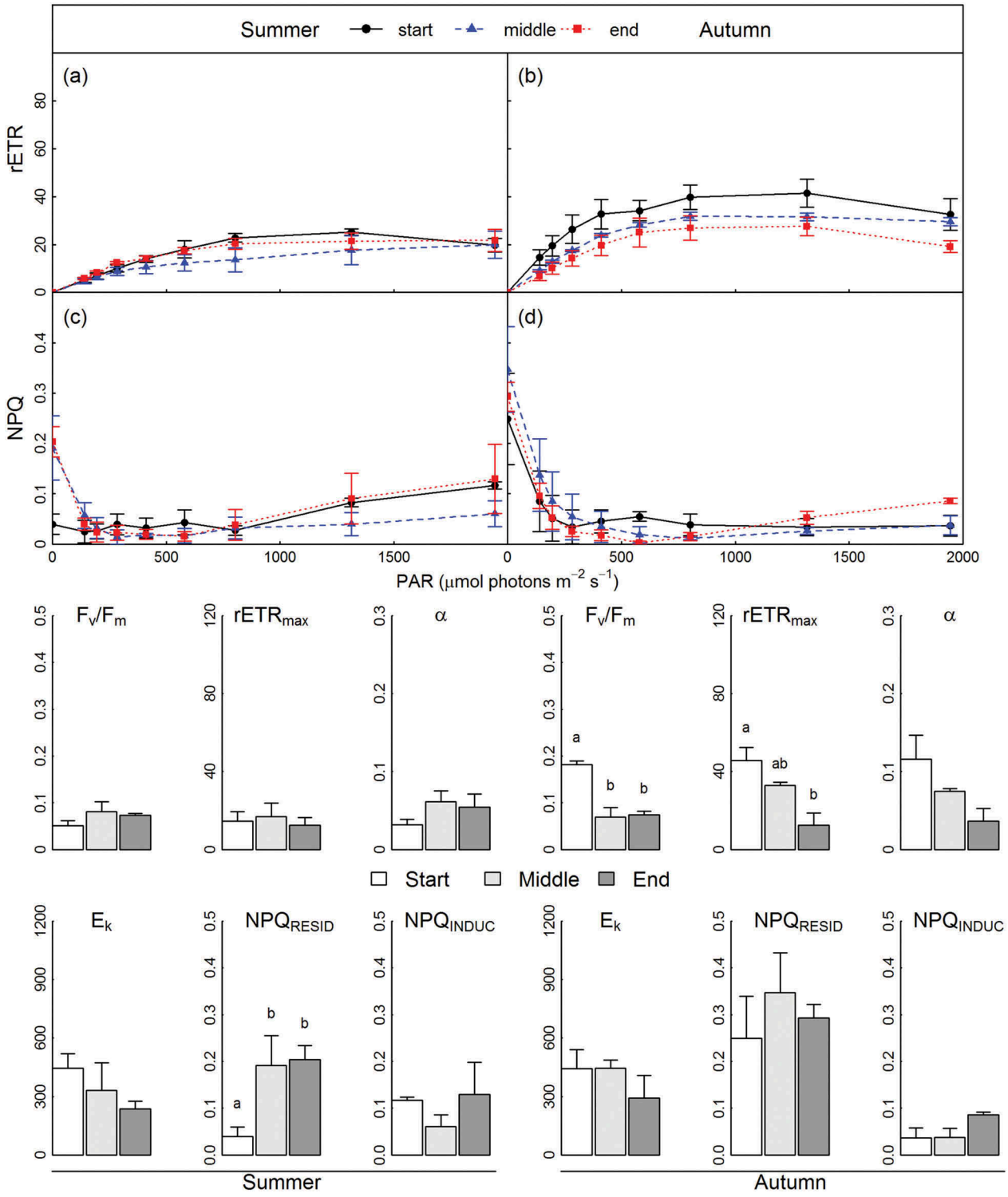

Fig. 10. *Corallina caespitosa* photophysiology in Comillas, northern Spain, in summer (left hand panels) and autumn (right hand panels) at the start (circles and solid lines/unshaded bars), middle (triangles and dashed lines/light grey bars) and end (squares and dotted lines/dark grey bars) of tidal emersion periods. Upper panels show the relative electron transport rates (rETR) (a & b) and non-photochemical quenching (NPQ) (c & d) determined over RLCs, with parameters derived from RLCs shown in bar plots below (mean ± SE, n = 3). Lower case letters denote homogeneous subsets determined from Tukey's HSD analysis in relation to the factor 'tide'.

NPQ can become exhausted during long or sudden exposure to excess irradiance, leading to damage of the D1 protein of PSII, decline in quantum efficiency and P_{max}, and ultimately chronic photoinhibition (Franklin & Forster, 1997). For low-light acclimated algae, increased light harvesting antenna can be a liability if high irradiance is encountered (Müller *et al.*, 2001; Beer *et al.*, 2014). Decreased *C. officinalis* α and $rETR_{max}$ in Iceland during autumn were therefore probably due to photoinhibition triggered by a combination of high irradiance and a low-light acclimated seasonal state. This was supported by *ex situ* RLCs, whereby low-light

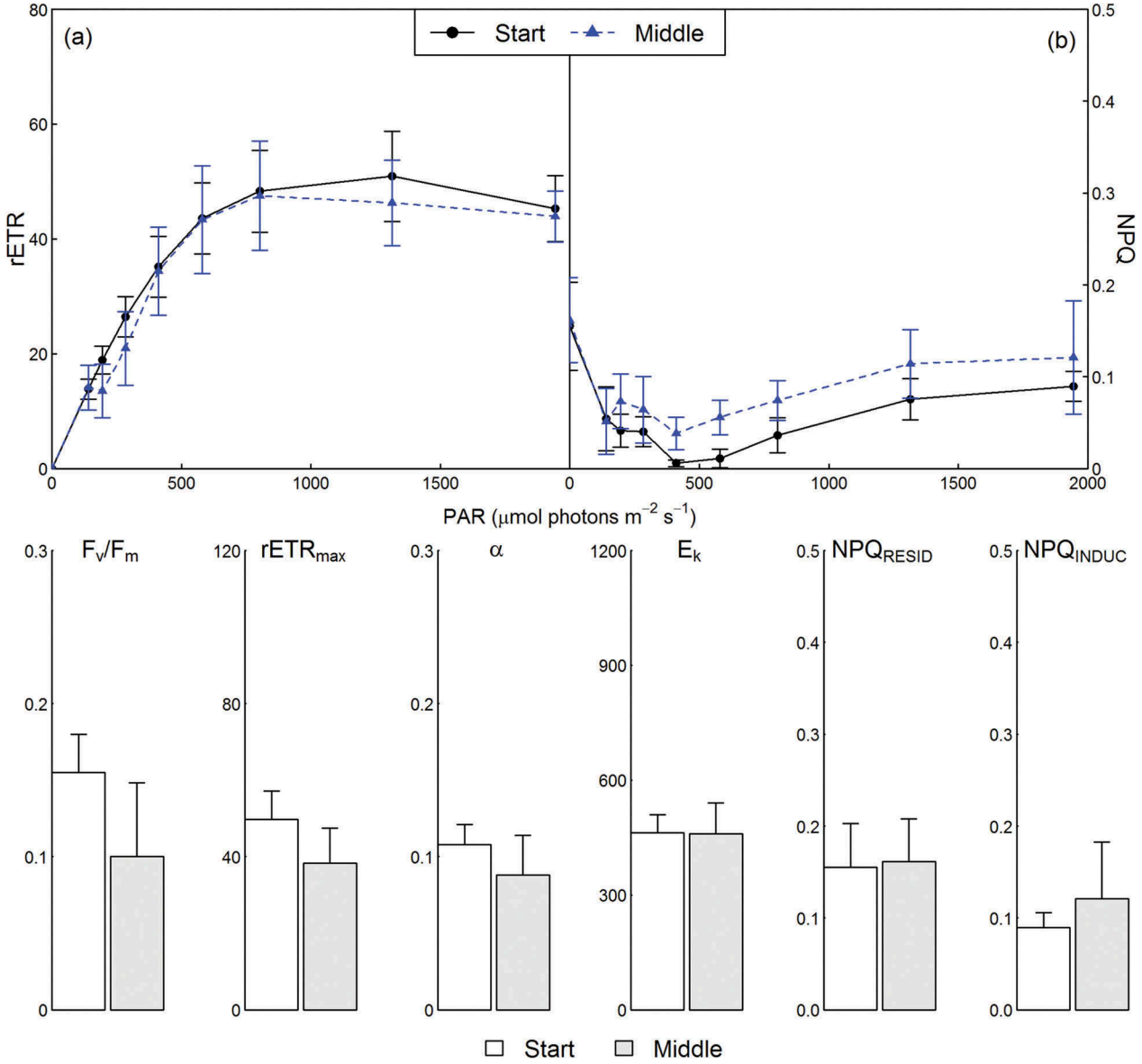

Fig. 11. *Corallina officinalis* photophysiology in Comillas, northern Spain, during summer at the start (circles and solid lines/unshaded bars) and middle (triangles and dashed lines/shaded bars) of tidal emersion periods. Upper panels show the relative electron transport rates (rETR) (a) and non-photochemical quenching (NPQ) (b) determined over RLCs, with parameters derived from RLCs shown in bar plots below (mean ± SE, n = 3).

photoacclimation of *C. officinalis* during autumn in Iceland was indicated by increased α in comparison with summer samples. Thus, whilst *in situ* RLCs provided assessment of the actual photochemistry under the prevailing abiotic conditions, *ex situ* RLCs following prolonged (>1 h) dark adaptation provided an important comparison allowing identification of the optimal photochemistry during different seasons.

Contrasting *in situ* and *ex situ* RLC findings revealed photostress as a suppressor of photosynthetic capacity for UK *C. officinalis* during summer. Following long-term dark adaptation, summer *C. officinalis* samples assessed *ex situ* achieved the same levels of $rETR_{max}$, α and E_k as autumn and winter samples from Combe Martin, in contrast to the reduced capacity for photochemistry recorded *in situ* during summer. Whilst differential photoacclimation was still indicated, given seasonal differences in the degree of NPQ induced across RLCs and the magnitude of recovery in quantum efficiency during darkness, data suggested that release from summer light-stress increased the capacity for photochemistry to that observed during other seasons. Similarly, *C. caespitosa* demonstrated increased α and $rETR_{max}$ during *ex situ* as compared with *in situ* summer RLCs in NSP, presumably due to release from high *in situ* light-stress. Previously, Richardson *et al.* (1983) questioned whether algae exhibiting photoacclimation via change in PSU number actually 'acclimate' to low irradiance conditions, or are merely stressed by higher light environments. Decreased F_v/F_m, indicative of increased stress in macroalgae (Maxwell & Johnson, 2000) was apparent *in situ* for both species during summer at all sites during the present study,

Table 6. Northern Spanish *Corallina caespitosa* (summer & autumn) and *C. officinalis* (summer only) *ex situ* photophysiology, as assessed by RLCs with recovery (n = 3 ± SE in parentheses).

	C. caespitosa		*C. officinalis*
	Summer	Autumn	Summer
RLC parameters			
F_v/F_m	0.29(0.02)	0.44(0.03)	0.35(0.03)
$rETR_{max}$	42.33(2.53)	77.55(3.94)	45.01(4.26)
α	0.07(0.01)	0.16(0.01)	0.12(0.01)
E_k	575.85(22.55)	482.68(49.3)	372.52(20.85)
	Relative Quantum Efficiency		
	Summer	Autumn	Summer
Recovery parameters			
End RLC	14.26(0.48)	16.13(1.88)	13.35(1.28)
End dark	88.43(6.47)	99.56(0.44)	89.43(6.03)
	NPQ		
	Summer	Autumn	Summer
End RLC	0.06(0.02)	0.19(0.07)	0.18(0.03)
End dark	0.01(0.01)	0(0)	0.04(0.03)

End RLC = relative quantum efficiency (%) or NPQ at the final RLC light step; End dark = the maximum recovery in relative quantum efficiency (%) and relaxation of NPQ achieved by the end of the dark recovery period.

indicating photo-stress impacts on *Corallina* photochemistry. However, alteration of pigment concentrations under different light environments has also been previously shown for *Corallina* species (e.g. Algarra *et al.*, 1991; Häder *et al.*, 1997; Kim *et al.*, 2013). Thus, whilst it is not possible to differentiate the relative roles of high light-stress and changes in pigment concentrations on the seasonal patterns in photophysiology observed during the present study, it is likely that both components play a governing role. Future research should aim to elucidate their relative contributions and, by extending observations over future seasonal cycles, confirm the re-occurrence of seasonal patterns in *Corallina* photochemistry characterized here.

Photoregulation via non-photochemical quenching

Non-photochemical quenching (NPQ) is highlighted by this study to be an important photoregulation mechanism utilized by *Corallina* species across the NE Atlantic, to prevent or minimize photoinhibition and maximize productivity in response to short-term changes in irradiance. NPQ is a common means by which to dissipate excess irradiance energy as heat in algae, preventing damage to photosystems (Hänelt *et al.*, 1993; Franklin & Forster, 1997; Lavaud & Lepetit, 2013). During the present study, maximal NPQ_{RESID}, representing active NPQ due to *in situ* irradiance, was coincident with maximal irradiance at all latitudes, whilst NPQ_{INDUC} at the end of RLCs was greatest under seasonal conditions of reduced irradiance. NPQ was therefore always available as a rapidly inducible means of photoregulation to prevent or reduce potential photoinhibition. Whilst NPQ is normally associated with energy dissipation as heat through the inter-conversion of xanthophyll pigments during the xanthophyll cycle (Demmig-Adams & Adams, 1996; Ralph & Gademann, 2005; Goss & Jakob, 2010), the existence of an operative xanthophyll cycle in red macroalgae remains unclear (see Goss & Jakob, 2010). Based on examination of pigment concentrations in the closely related *Ellisolandia elongata* (as *Corallina elongata*) from northern Spain, Esteban *et al.* (2009) concluded that if a xanthophyll cycle exists in *E. elongata*, it must represent a truncated version of the violaxanthin–antheraxanthin–zeaxanthin (V-A-Z) cycle, restricted to the inter-conversion of A and Z, as shown for *Gracilaria gracilis* and *G. multipartita*. Whilst the present study cannot demonstrate whether NPQ recorded was directly linked to the inter-conversion of xanthophyll pigments in *Corallina*, our data highlight that rapid photoregulation through induction of NPQ over 30 s light steps was possible for both species, at all latitudes, with rapid reversal of NPQ apparent in darkness.

Previously, Williamson *et al.* (2014*b*) demonstrated that the ability of UK *Corallina* populations to photoregulate via NPQ over tidal emersion periods was related to the seasonal state of photoacclimation. During summer, *rETRmax* was maintained or increased over tidal emersion due to rapid and effective photoregulation, whilst during winter, photophysiology was sensitive to relatively small changes in irradiance due to a low-light-acclimated state and less effective photoregulation (Williamson *et al.*, 2014*b*). Findings of the present study corroborate Williamson *et al.* (2014*b*), demonstrating increased sensitivity of *in situ* photophysiology over autumn tidal emersion periods, as compared with summer, for both Icelandic *C. officinalis*, and northern Spanish *C. caespitosa* populations. Lack of significant tidal variability in photophysiology of *C. officinalis* examined from the very lower intertidal in northern Spain probably reflects the shorter duration of emersion, and thus reduced emersion stress, experienced at this shore height (Williamson *et al.*, 2014*b*).

Additional to seasonal variability, the present study further indicates latitudinal patterns in the photoregulation capacity of *Corallina* across the NE Atlantic. The faster NPQ returns to 0 in darkness is an indicator of a plant's tolerance to high light (Ralph & Gademann, 2005). By monitoring relaxation kinetics after *ex situ* RLCs it was thus possible to examine recovery from light exposure, allowing the various components of NPQ to be distinguished. The component of NPQ which relaxes quickly (seconds–minutes) is associated with the removal of energy-dependent NPQ (*qE*), and is linked to relaxation of the proton gradient across the thylakoid membrane (Ralph & Gademann, 2005). In contrast, a slower relaxation of NPQ (>10 min, up to hours), is associated with photoinhibition (*qI*) and changes in energy distribution in favour of PSII (Ralph & Gademann, 2005). *qE* was shown here to be the major component of *Corallina* NPQ, with rapid relaxation to 0 by a maximum of 160 s of darkness observed during summer and autumn in the UK and northern Spain for both *Corallina* species. In contrast, *qI* was identified for Icelandic *C. officinalis* during both summer and autumn, given the persistence of NPQ following 17.5 min of darkness. Recovery of quantum efficiency by the end of dark periods further showed latitudinal gradients, with the greatest recovery observed in lower relative to higher latitudes, in all seasons. *Corallina* populations thus demonstrated an increased susceptibility to photostress, and reduced capacity for photoregulation, with increasing latitude across the NE Atlantic.

Species with an extended latitudinal distribution can be exposed to high environmental variability that may promote phenotypic plasticity and/or ecotype differentiation as an adaptive response to temporal and spatial variation (Lynch & Gabriel, 1987). Given that the net amount of solar radiation reaching the earth's surface decreases with increasing latitude (Beaugrand, 2014), data may reflect low-light photoacclimation (or photoadaptation) of higher latitude *Corallina* populations across the NE Atlantic, with consequent increases in sensitivity to photostress relative to lower latitude populations. This may be further exacerbated by low temperature restrictions on enzymatic recovery processes at higher latitudes, which can mimic the impacts of high-light stress (Ensminger *et al.*, 2006; Huner *et al.*, 1996). In this respect, the capacity for NE Atlantic *Corallina* populations to effectively photoregulate may decrease with increasing latitude due to differential photoacclimation coupled with low-temperature restrictions to physiology.

Interspecific differences in photochemistry

Data highlighted highly conserved photophysiology between *C. officinalis* and *C. caespitosa*, consistent with the findings of Williamson *et al.* (2014*b*). For example, seasonal patterns in *in situ* photophysiology in the UK were almost identical between the two species, with no significant difference in F_v/F_m, $rETR_{max}$, α or E_k observed. Furthermore, where interspecific differences were apparent *in situ*, these reflected local responses to differential abiotic stress given their respective positions on the shore (Varela *et al.*, 2006), and were absent with removal for *ex situ* analyses of photochemistry. Known differences in the global distributions of the *Corallina* species studied here (Williamson *et al.*, 2015) do not, therefore, appear to relate to differential capacity for photochemistry. As such, further research is required to examine the physiological mechanisms underlying interspecific differences within the genus *Corallina*.

Disclosure statement

No potential conflict of interest was reported by the authors.

Funding

This work was funded by the NERC grant (NE/H025677/1).

Author contributions

C. Williamson, R. Perkins, M Yallop and J. Brodie: original concept and study design; All authors: field support, field sampling and manuscript preparation.

Supplementary information

The following supplementary material is accessible via the Supplementary Content tab on the article's online page at https://doi.org/10.1080/09670262.2018.1442586.

Supplementary table 1. Analysis of variance of UK *C. officinalis* and *C. caespitosa* seasonal photophysiology.

Supplementary table 2. Analysis of variance and t-test analysis of UK *C. officinalis* and *C. caespitosa ex-situ* photophysiology parameters in relation to the factor 'season'.

Supplementary fig. 1. *Ex-situ* rapid light response curves with recovery for *C. officinalis* during summer and autumn at Þorlákshöfn, Iceland, showing (a) relative electron transport rates (rETR) over the induction phase of RLCs, and (b) relative quantum efficiency (RQE) and (c) non-photochemical quenching (NPQ) over the induction and dark recovery phases.

Supplementary fig. 2. *Ex-situ* rapid light response curves with recovery for *C. caespitosa* during summer and autumn at Comillas, northern Spain, showing (a) relative electron

transport rates (rETR) over the induction phase of RLCs, and (b) relative quantum efficiency (RQE) and (c) non-photochemical quenching (NPQ) over the induction and dark recovery phases.

Supplementary fig. 3. *Ex-situ* rapid light response curves with recovery for *C. officinalis* during summer at Comillas, northern Spain, showing (a) relative electron transport rates (rETR) over the induction phase of RLCs, and (b) relative quantum efficiency (RQE) and (c) non-photochemical quenching (NPQ) over the induction and dark recovery phases.

ORCID

César Peteiro http://orcid.org/0000-0003-0698-3573

References

Algarra, P., Delavina, G. & Niell, J. (1991). Effects of light quality and irradiance level interactions on short-term pigment response of the red alga *Corallina elongata*. *Marine Ecology Progress Series*, **74**: 27–32.

Bates, D., Maechler, M., Bolker, B. & Walker, S. (2013). lme4: Linear mixed-effects models using Eigen and S4. R package.

Beaugrand, G. (2014). *Marine Biodiversity, Climatic Variability and Global Change*. Routledge, Abingdon.

Beer, S., Bjork, M. & Beardall, J. (2014). *Photosynthesis in the Marine Environment*. Wiley-Blackwell, Ames, IA.

Brodie, J., Walker, R.H., Williamson, C. & Irvine, L.M. (2013). Epitypification and redescription of *Corallina officinalis* L., the type of the genus, and *C. elongata* Ellis et Solander (Corallinales, Rhodophyta). *Cryptogamie, Algologie*, **34**: 49–56.

Brodie, J., Williamson, C.J., Barker, G., Walker, R.H., Briscoe, A., & Yallop, M. (2016). Characterising the microbiome of Corallina officinalis, a dominant calcified intertidal red Alga. FEMS Microbiology Ecology **92**: fiw110.

Consalvey, M., Perkins, R.G., Paterson, D.M. & Underwood, G.J.C. (2005). PAM Fluorescence: a beginners guide for benthic diatomists. *Diatom Research*, **20**: 1–22.

Cosgrove, J. & Borowitzka, M.A. (2011) Chlorophyll fluorescence terminology: an introduction. In *Chlorophyll a Fluorescence in Aquatic Sciences: Methods and Applications* (Suggett, D.J., Prášil, O. & Borowitzka, M. A., editors), 1–17. Springer, Dordrecht.

Coull, B.C. & Wells, J.B.J. (1983). Refuges from fish predation – experiments with phytal meiofauna from the New Zealand rocky intertidal. *Ecology*, **64**: 1599–1609.

Davison, I. & Pearson, G. (1996). Stress tolerance in intertidal seaweeds. *Journal of Phycology*, **32**: 197–211.

Demmig-Adams, B. & Adams, W.W. (1996). Xanthophyll cycle and light stress in nature: uniform response to excess direct sunlight among higher plant species. *Planta*, **198**: 460–470.

Dera, J. & Gordon, H.R. (1968). Light field fluctuations in photic zone. *Limnology and Oceanography*, **13**: 697–699.

Egilsdottir, H., Noisette, F., Noël, L.M.-L.J., Olafsson, J. & Martin, S. (2013). Effects of pCO_2 on physiology and skeletal mineralogy in a tidal pool coralline alga *Corallina elongata*. *Marine Biology*, **160**: 2103–2112.

Eilers, P.H.C. & Peeters, J.C.H. (1988). A model for the relationship between light intensity and the rate of photosynthesis in phytoplankton. *Ecological Modelling*, **42**: 199–215.

Ensminger, I., Busch, F. & Huner, N.P.A. (2006). Photostasis and cold acclimation: sensing low temperature through photosynthesis. *Physiologia Plantarum*, **126**: 28–44.

Esteban, R., Martínez, B., Fernández-Marín, B., Becerril, J. M. & García-Plazaola, J.I. (2009). Carotenoid composition in Rhodophyta: insights into xanthophyll regulation in *Corallina elongata*. *European Journal of Phycology*, **44**: 221–230.

Falkowski, P.G. & LaRoche, J. (1991). Acclimation to spectral irradiance in algae. *Journal of Phycology*, **27**: 8–14.

Franklin, L.A. & Forster, R.M. (1997). The changing irradiance environment: consequences for marine macrophyte physiology, productivity and ecology. *European Journal of Phycology*, **32**: 207–232.

Goss, R. & Jakob, T. (2010). Regulation and function of xanthophyll cycle-dependent photoprotection in algae. *Photosynthesis Research*, **106**: 103–122.

Häder, D-P., Lebert, M., Flores-Moya, A., Jiménez, C., Mercado, J., Salles, S., Aguilera, J. & Figueroa, F.L. (1997). Effects of solar radiation on the photosynthetic activity of the red alga *Corallina elongata* Ellis et Soland. *Journal of Photochemistry and Photobiology B: Biology*, **37**: 116–202.

Häder, D-P., Lebert, M, & Helbling E.W. (2003). Effects of solar radiation on the Patagonian Rhodophyte *Corallina officinalis* (L.). *Photosynthesis Research*, **78**: 119–132.

Hänelt, D., Huppertz. K & Nultsch, W. (1993). Daily course of photosynthesis and photoinhibition in marine macroalgae investigated in the laboratory and field. *Marine Ecology Progress Series*, **97**: 31–37.

Henley, W.J. & Ramus, J. (1989). Time course of physiological response of *Ulva rotundata* to growth irradiance transitions. *Marine Ecology Progress Series*, **54**: 171–177.

Hofmann, L., Yildiz, G., Hanelt, D. & Bischof, K. (2012). Physiological responses of the calcifying rhodophyte, *Corallina officinalis* (L.), to future CO_2 levels. *Marine Biology*, **159**: 783–792.

Huner, N.P.A., Maxwell, D.P., Gray, G.R., Savitch, L.V., Krol, M., Ivanov, A.G. & Falk, S. (1996). Sensing environmental change: PSII excitation pressure and redox signalling. *Physiologia Plantarum*, **98**: 358–364.

Huot, Y. & Babin, M. (2011). Overview of fluorescence protocols: theory, basic concepts and practice. In *Chlorophyll a Fluorescence in Aquatic Sciences: Methods and Applications* (Suggett, D.J., Prášil, O. & Borowitzka, M.A., editors), 31–74. Springer, Dordrecht.

Johansen, H.W. (1981). *Coralline Algae: A First Synthesis*. CRC Press, Boca Raton, FL.

Kelaher, B.P. (2002). Influence of physical characteristics of coralline turf on associated macrofaunal assemblages. *Marine Ecology Progress Series*, **232**: 141–148.

Kelaher, B.P. (2003). Changes in habitat complexity negatively affect diverse gastropod assemblages in coralline algal turf. *Oecologia*, **135**: 431–441.

Kim, J.H., Lam, S.M.N. & Kim, K.Y. (2013). Photoacclimation strategies of the temperate coralline alga *Corallina officinalis*: a perspective on photosynthesis, calcification, photosynthetic pigment contents and growth. *Algae*, **28**: 355–363.

Lavaud, J. & Lepetit, B. (2013). An explanation for the inter-species variability of the photoprotective non-photochemical chlorophyll fluorescence quenching in diatoms. *Biochimica et Biophysica Acta – Bioenergetics*, **1827**: 294–302.

Lobban, C.S. & Harrison, P.J. (1994). *Seaweed Ecology and Physiology*. Cambridge University Press, New York, NY.

Lynch, M. & Gabriel, W. (1987). Environmental tolerance. *American Naturalist*, **129**: 203–208.

Maxwell, K. & Johnson, G.N. (2000). Chlorophyll fluorescence – a practical guide. *Journal of Experimental Botany*, **51**: 659–668.

Müller, P., Xiao-ping, L & Niyogi, K.K. (2001). Update on photosynthesis non-photochemical quenching: a response to excess light energy. *Plant Physiology*, **125**: 1558–1566.

Noisette, F., Egilsdottir, H., Davoult, D. & Martin, S. (2013). Physiological responses of three temperate coralline algae from contrasting habitats to near-future ocean acidification. *Journal of Experimental Marine Biology and Ecology*, **448**: 179–187.

Perkins, R.G., Mouget. J-L., Lefebvre, S. & Lavaud, J. (2006). Light response curve methodology and possible implications in the application of chlorophyll fluorescence to benthic diatoms. *Marine Biology*, **149**: 703–712.

Perkins, R.G., Kromkamp, J.C., Serôdio, J., Lavaud, J., Jesus, B., Mouget, J.L., Lefebvre, S. & Forster, R.M. (2010). The application of variable chlorophyll fluorescence to microphytobenthic biofilms. In *Chlorophyll a Fluorescence in Aquatic Sciences: Methods and Applications* (Suggett, D.J., Prášil, O. & Borowitzka, M. A., editors), 237–275. Springer, Dordrecht.

Perkins, R.G., Williamson, C.J., Brodie, J., Barille, L., Launeau, P., Lavaud, J., Yallop, M.L. & Jesus, B. (2016). Microspatial variability in community structure and photophysiology of calcified macroalgal microbiomes revealed by coupling of hyperspectral and high-resolution fluorescence imaging. *Scientific Reports*, **6**: 22343.

R Core Team (2014). *R: A Language and Environment for Statistical Computing*. R Foundation for Statistical Computing, Vienna.

Ralph, P.J. & Gademann, R. (2005). Rapid light curves: a powerful tool to assess photosynthetic activity. *Aquatic Botany*, **82**: 222–237.

Ramus, J. (1981). The capture and transduction of light energy. In *The Biology of Seaweeds* (Lobban, C.S. & Wynee, M.J., editors), 458–492. Blackwell Scientific, Oxford.

Richardson, K., Beardall, J. & Raven, J.A. (1983). Adaptation of unicellular algae to irradiance – an analysis of strategies. *New Phytologist*, **93**: 157–191.

Serôdio, J., Cruz, S., Vieira, S. & Brotas, V. (2005). Non-photochemical quenching of chlorophyll fluorescence and operation of the xanthophyll cycle in estuarine microphytobenthos. *Journal of Experimental Marine Biology and Ecology*, **326**: 157–169.

Varela, D.A., Santelices, B., Correa, J.A. & Arroyo, M.K. (2006). Spatial and temporal variation of photosynthesis in intertidal *Mazzaella laminarioides* (Bory) Fredericq (Rhodophyta, Gigartinales). *Journal of Applied Phycology*, **18**: 827–838.

Venables, W.N. & Ripley, B.D. (2002). *Modern Applied Statistics with S*. 4th ed. Springer, New York, NY.

Williamson, C.J., Najorka, J., Perkins, R., Yallop, M.L. & Brodie, J. (2014a). Skeletal mineralogy of geniculate corallines: providing context for climate change and ocean acidification research. *Marine Ecology Progress Series*, **513**: 71–84.

Williamson, C.J., Brodie, J., Goss, B., Yallop, M.L., Lee, S. & Perkins, R. (2014b). *Corallina* and *Ellisolandia* (Corallinales, Rhodophyta) photophysiology over daylight tidal emersion: interactions with irradiance, temperature and carbonate chemistry. *Marine Biology*, **161**: 2051–2068.

Williamson, C.J., Walker, R.H., Robba, L., Yesson, C., Russell, S., Irvine, L.M. & Brodie, J. (2015). Toward resolution of species diversity and distribution in the calcified red algal genera *Corallina* and *Ellisolandia* (Corallinales, Rhodophyta). *Phycologia*, **54**: 2–11.

Williamson, C.J., Perkins, R., Voller, M., Yallop, M.L. & Brodie, J. (2017). The regulation of coralline algal physiology, an in-situ study of *Corallina officinalis* (Corallinales, Rhodophyta). *Biogeosciences*, **14**: 4485–4498.